The Waisman Laboratory for Brain Imaging and Behavior

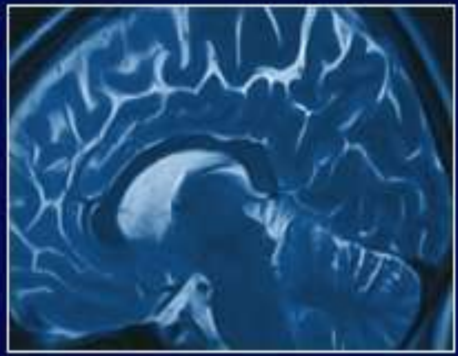

University of Wisconsin SCHOOL OF MEDICINE AND PUBLIC HEALTH

Heat kernel smoothing, hot spots conjecture and Fiedler vector

Moo K. Chung

University of Wisconsin-Madison

www.stat.wisc.edu/~mchung

2017 September 5, Casa Mexicana Oaxaca

Abstracts

The second eigenfunction of the Laplace-Beltrami operator (often called Fiedler vector in discrete settings) follows the pattern of the overall shape of an object. This geometric property is well known and used for various applications including mesh processing, feature extraction, manifold learning, spectral embedding and the minimum linear arrangement problem. Surprisingly, this geometric property has not been precisely formulated yet. This problem is directly related to the somewhat obscure hot spots conjecture in differential geometry that postulates the behavior of heat diffusion near boundary. The aim of the talk is to discuss and raise the awareness of the problem. As an application of the hot spots conjecture, we show how the second eigenfunction alone can be used for shape modeling of elongated anatomical structures such as hippocampus and mandible, and determining the diameter of large-scale brain networks. This talk is based on Chung et al. 2015 Medical Image Analysis 22:63-76.

Acknowledgements

Yuan Wang, Houri Voperian, Andrew Alexander, Seth Pollack, Richard Davidson

University of Wisconsin-Madison

Seong Ho Seo *Seoul National University*

NIH funding: EB022856, MH098098, MH061285

Diffusion smoothing

The Canadian Journal of Statistics
Vol. 28, No. 2, 2000, Pages 225–240
La revue canadienne de statistique

Differential equation models for statistical functions[1]

James O. RAMSAY

Diffusion smoothing
with boundary condition

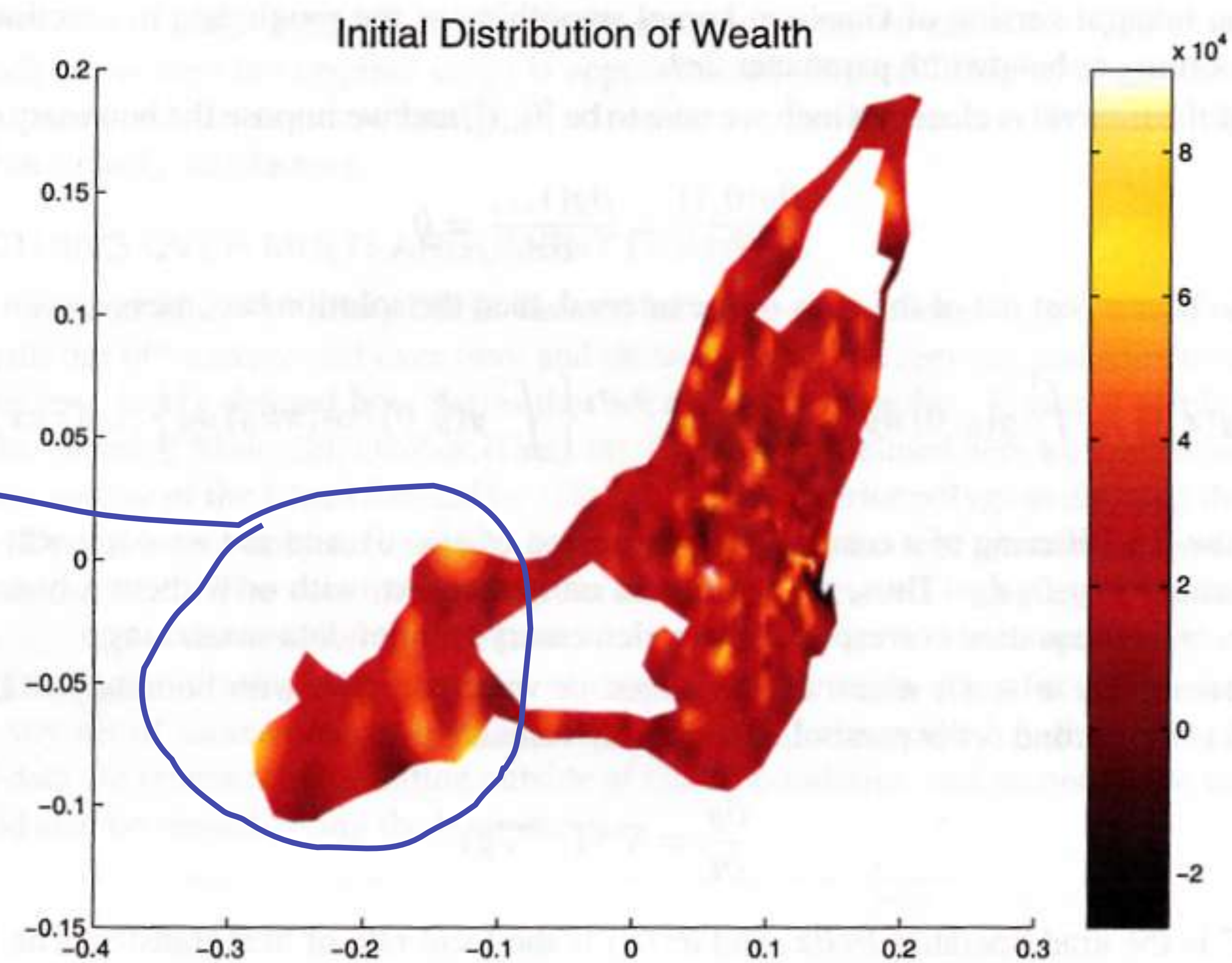

FIGURE 10: The distribution of wealth on the Island of Montréal. This defines the initial state $g(x, 0)$ of the system described by partial differential equation (15) and boundary condition (16).

Diffusion Smoothing in Brain Imaging

Moo K. Chung[1], Keith J. Worsley[1], Jonathan Taylor[1], James O. Ramsay[2]
[1] *Department of Mathematics and Statistics,* [2] *Department of Psychology*
McGill University
Montreal, Québec, Canada H3A 2K6
Web: `http://www.math.mcgill.ca/chung`

Gaussian kernel smoothing has been widely used in smoothing 2D or 3D images such as magnetic resonance imaging (MRI), positron emission tomography (PET). An integral version of isotropic Gaussian kernel smoothing of the function $f(\mathbf{x}), \mathbf{x} = (x_1, \cdots, x_n) \in \Re^n$ with

2001, Proceedings of the 53rd Session of the International Statistical Institute

$$\Delta F = \frac{1}{|g|^{1/2}} \sum_{i,j=1}^{n} \frac{\partial}{\partial u^i}\Big(|g|^{1/2} g^{ij} \frac{\partial F}{\partial u^j}\Big), \tag{3}$$

where $|g| = \det(g_{ij})$ and $g^{-1} = (g^{ij})$. Using the finite element method, we estimate (3) on the triangular mesh of the brain surfaces (Chung, 2001). Let $F(\mathbf{p}_i)$ be the data on the i-th node $\mathbf{p}_i$ in the triangular mesh. If $\mathbf{p}_1$,...,$\mathbf{p}_m$ are m-neighboring nodes around the central node $\mathbf{p}$, the Laplace-Beltrami operator is estimated as $\widehat{\Delta F}(\mathbf{p}) = \sum_{i=1}^{m} w_i(F(\mathbf{p}_i) - F(\mathbf{p}))$ with the weights $w_i = (\cot\theta_i + \cot\phi_i)/|T|$, where θ_i and ϕ_i are the two angles opposite to the edge connecting $\mathbf{p}_i$ and $\mathbf{p}$, and $|T|$ is the sum of the areas of the m-incident triangles at $\mathbf{p}$. Afterwards, (2) is

FEM-based discretization of LB-operator

$$\Delta_X F = \frac{1}{|g|^{1/2}} \sum_{i,j=1}^{2} \frac{\partial}{\partial u^i}\left(|g|^{1/2} g^{ij} \frac{\partial F}{\partial u^j}\right)$$

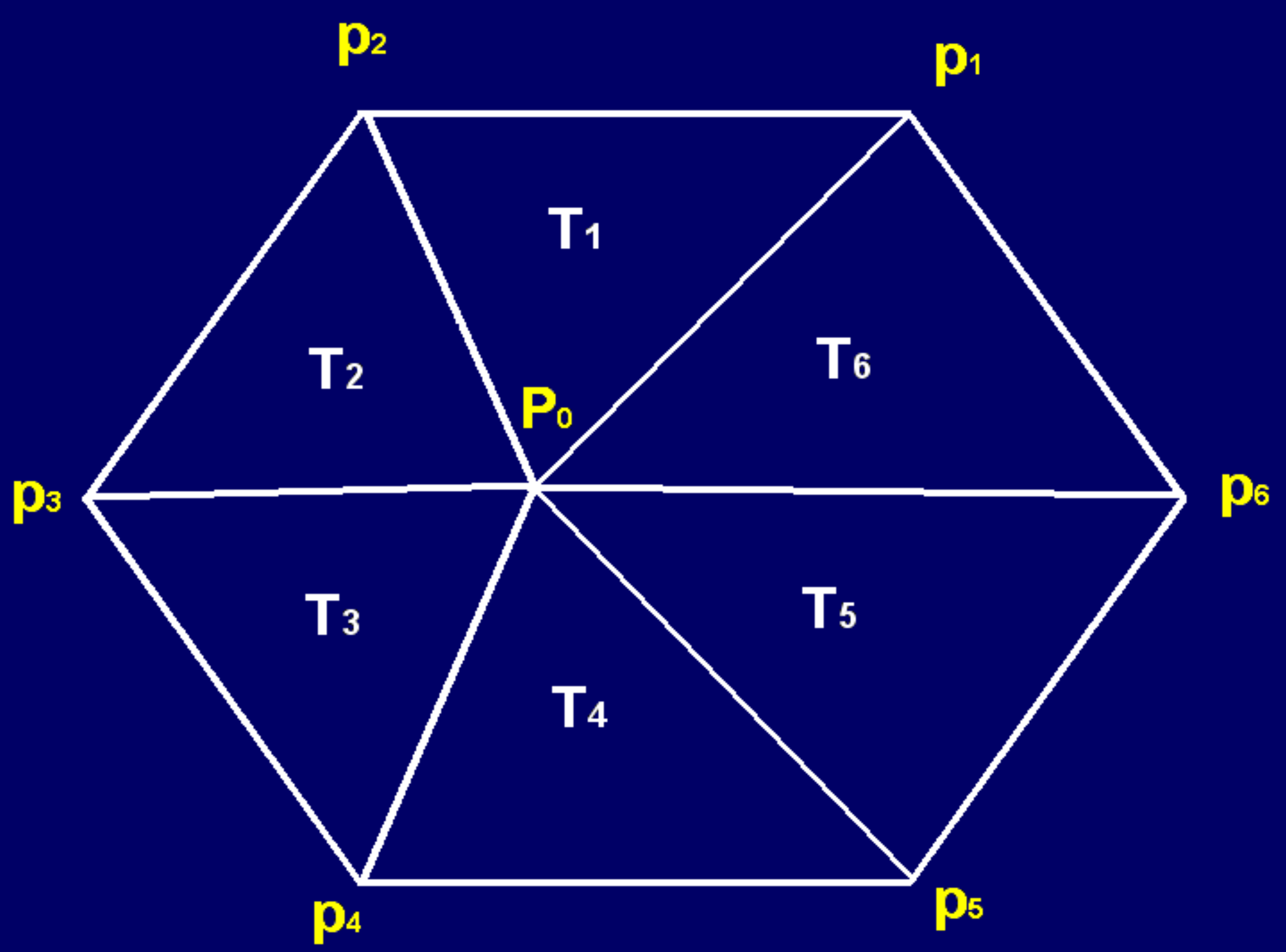

$$w_i = \frac{\cot\theta_i + \cot\phi_i}{\sum_{i=1}^{m} |T_i|}$$

$$\widehat{\Delta} F(p_0) = w_0 F(p_0) + w_1 F(p_1) + \cdots + w_m F(p_m)$$

Proved in Lopez-Perez et al, 2004, ECCV

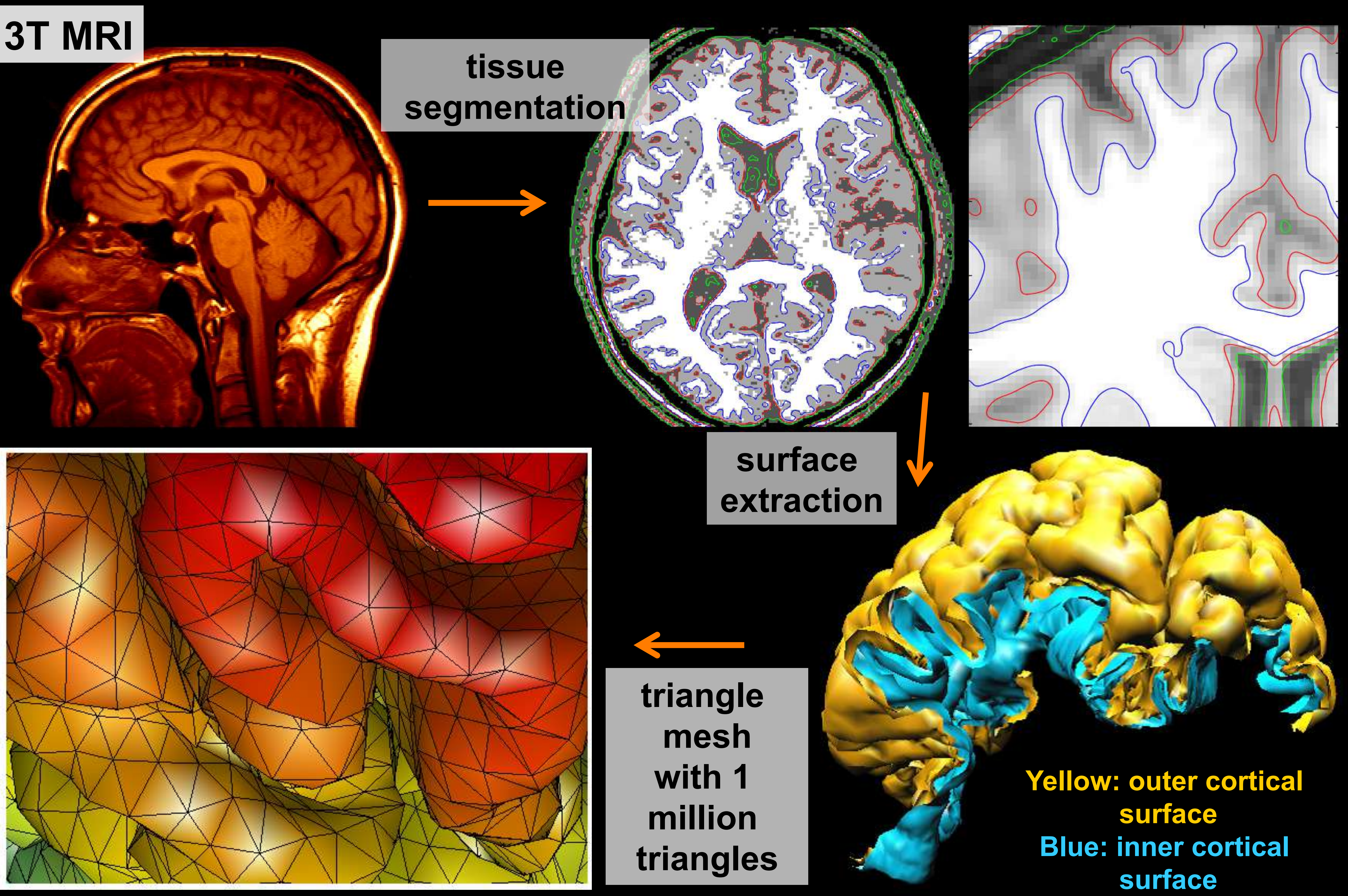
3T MRI
tissue segmentation
surface extraction
triangle mesh with 1 million triangles
Yellow: outer cortical surface
Blue: inner cortical surface

5mm FWHM Diffusion Smoothing

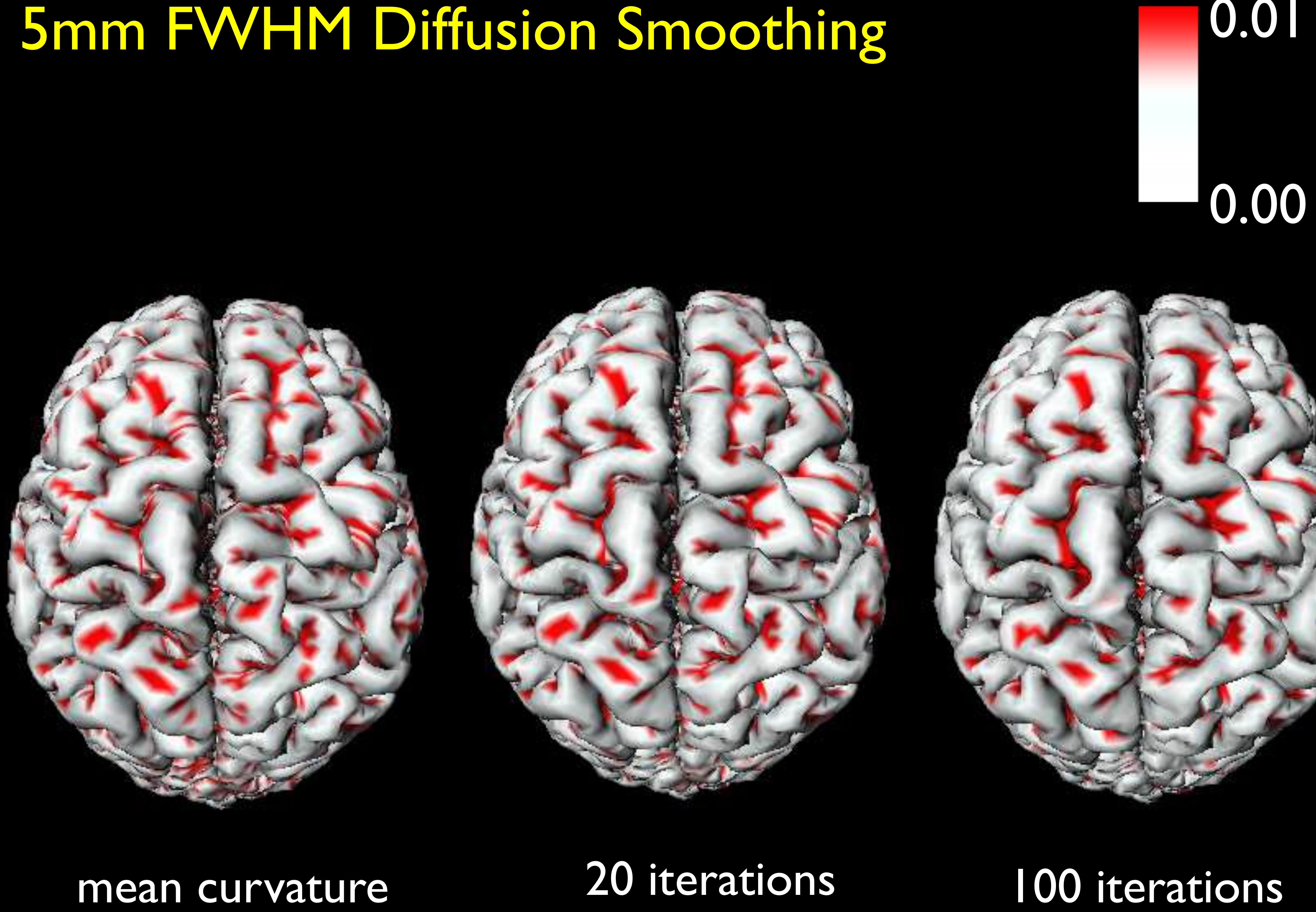

Matlab code: http://brainimaging.waisman.wisc.edu/~chung/diffusion

Heat kernel smoothing

Smoothing in manifold

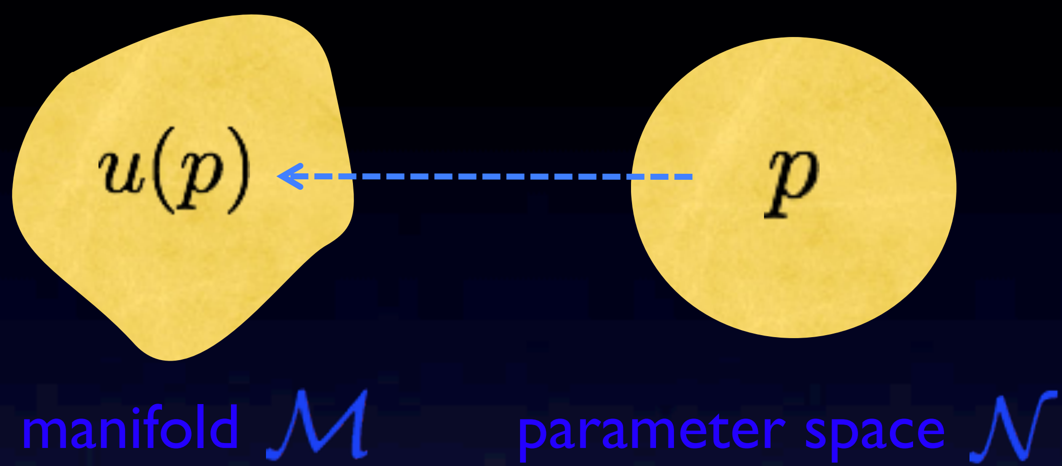

Anatomical manifold $\mathcal{M} \in \mathbb{R}^d$

Parameter space $\mathcal{N} \in \mathbb{R}^m$

Hilbert space $L^2(\mathcal{N})$ with inner product

$$L^2(\mathcal{M}) \qquad \langle g_1, g_2 \rangle = \int_{\mathcal{N}} g_1(p) g_2(p) \mu(p)$$

Self-adjoint operator $\mathcal{L}$

$$\langle \mathcal{L} g_1, g_2 \rangle = \langle g_1, \mathcal{L} g_2 \rangle$$

Basis function

$$\mathcal{L} \psi_j = \lambda_j \psi_j$$

Analytic approach to heat kernel smoothing

t = scale, bandwidth, diffusion time

Input signal

PDE: $\partial_t g + \mathcal{L} g = 0, g(p, t=0) = f(p)$

Analytic representation

Weighed Fourier series $g(p,t) = \sum_{j=0}^{\infty} e^{-\lambda_j t} \langle f, \psi_j \rangle \psi_j(p)$

Kernel smoothing $= \int_{\mathcal{N}} K_t(p,q) f(q) \, d\mu(q)$

Chung et al., 2007. IEEE Transactions on Medical Imaging 26:566-581

Heat kernel smoothing on manifold

$$K_\sigma * X(p) = \sum_{j=0}^{\infty} e^{-\lambda_j \sigma} X_j \psi_j(p)$$

$$X_j = \langle X, \psi_j \rangle$$

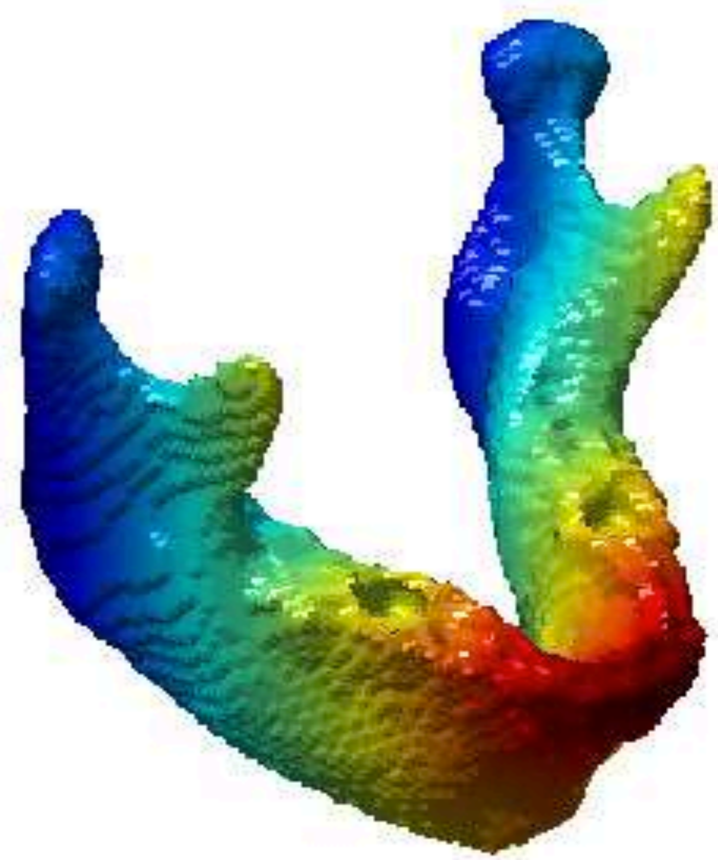

X-coordinate

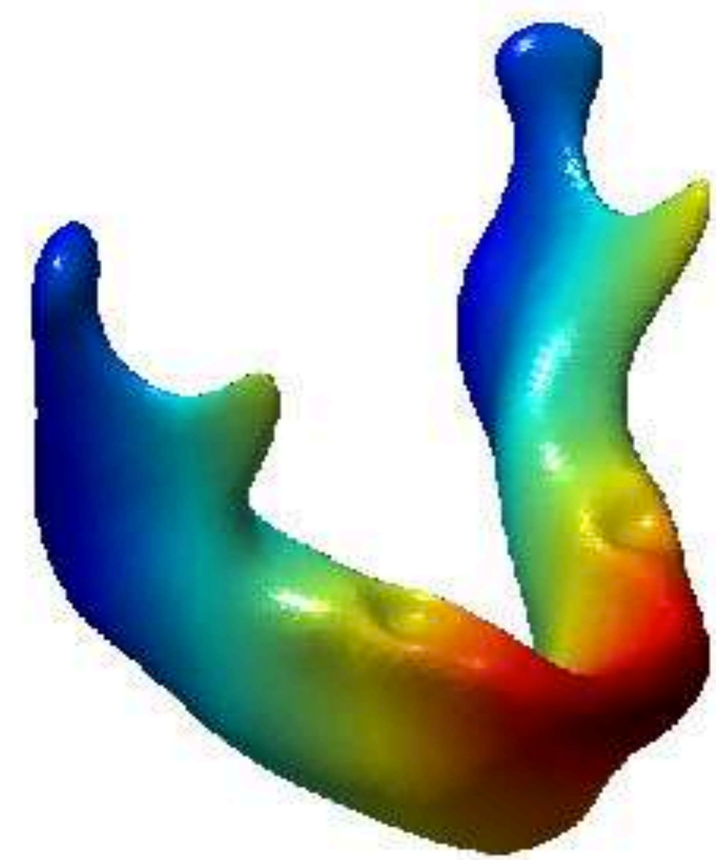

smoothed with bandwidth 10
and 1269 eigenfunctions

Discretize basis functions via FEM

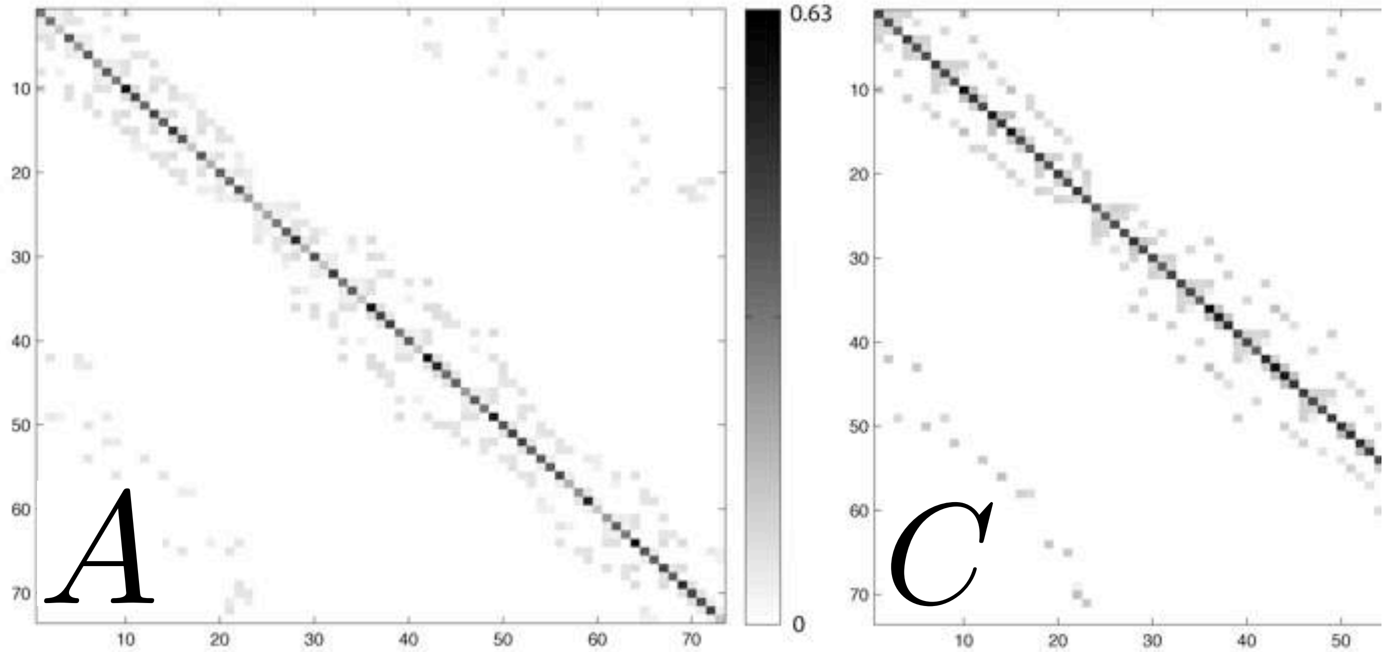

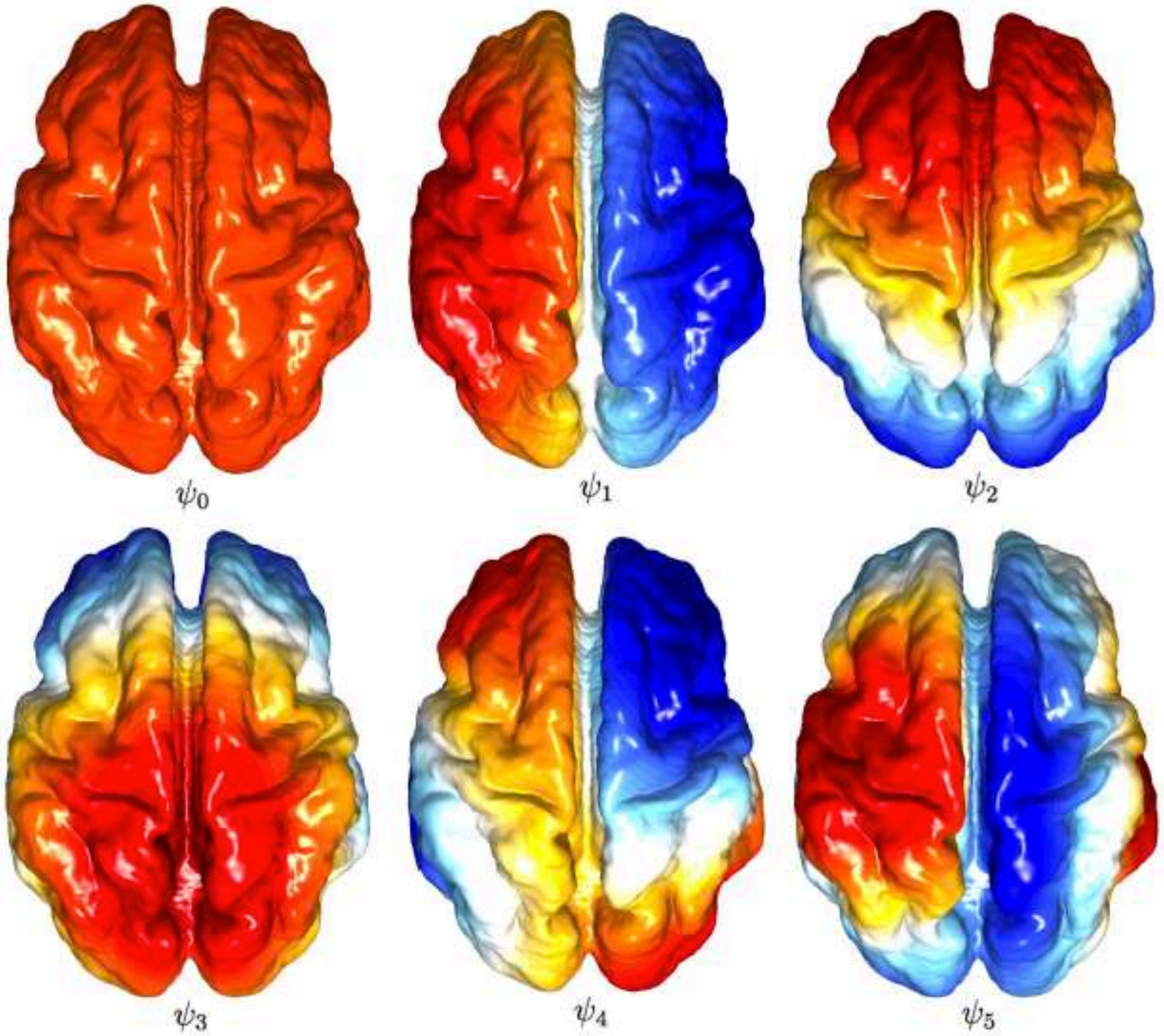

$$\Delta f = \lambda f \quad \longrightarrow \quad C\psi = \lambda A\psi$$

MATLAB code:

http://brainimaging.waisman.wisc.edu/~chung/lb

Functional approach to heat kernel smoothing

$$K_\sigma * X(p) = \sum_{j=0}^{\infty} e^{-\lambda_j \sigma} X_j \psi_j(p)$$

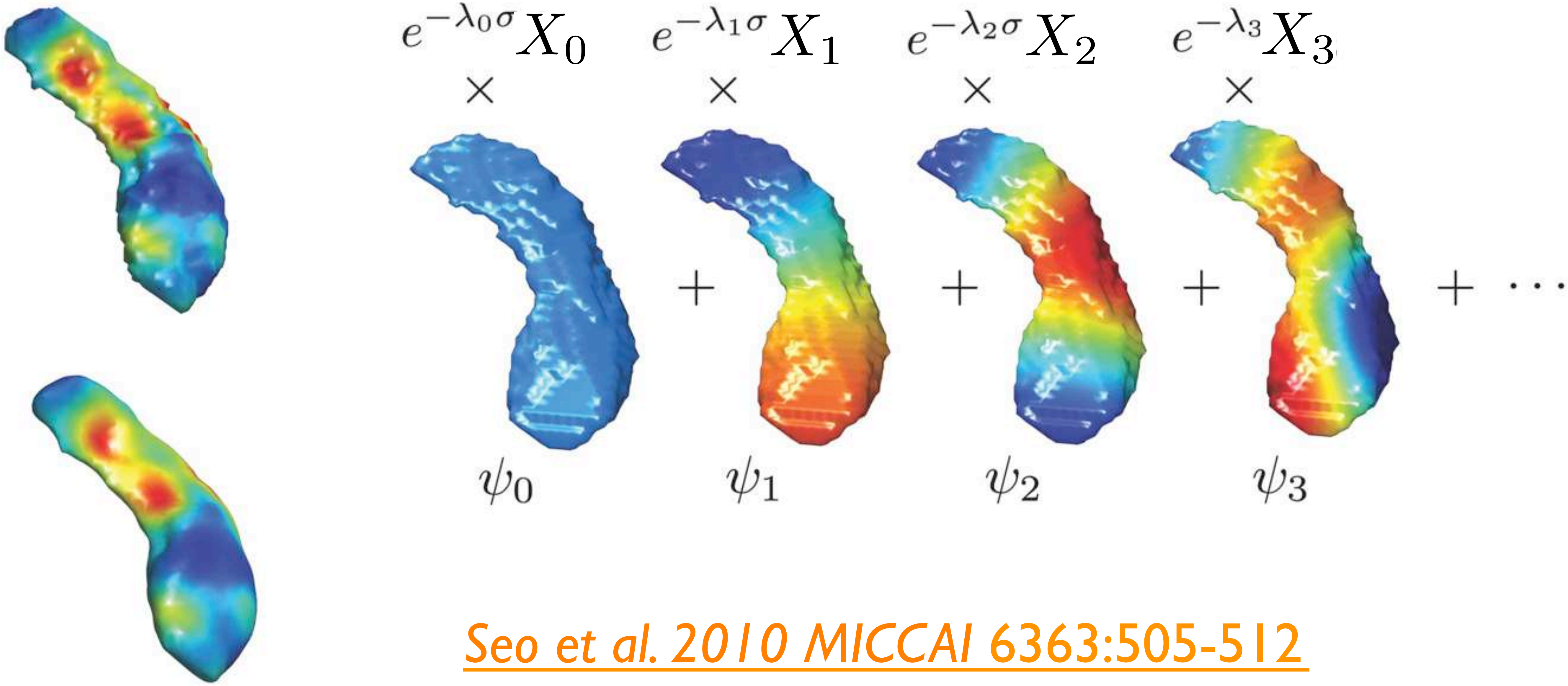

Seo et al. 2010 MICCAI 6363:505-512

Chung et al. 2015 Medical Image Analysis 22:63-76

Hot Spots Conjecture

Chung et al. 2011 Lecture Notes in Computer Science (LNCS). 7009:225-232

Motivation: determine the length of mandible

+ heat source

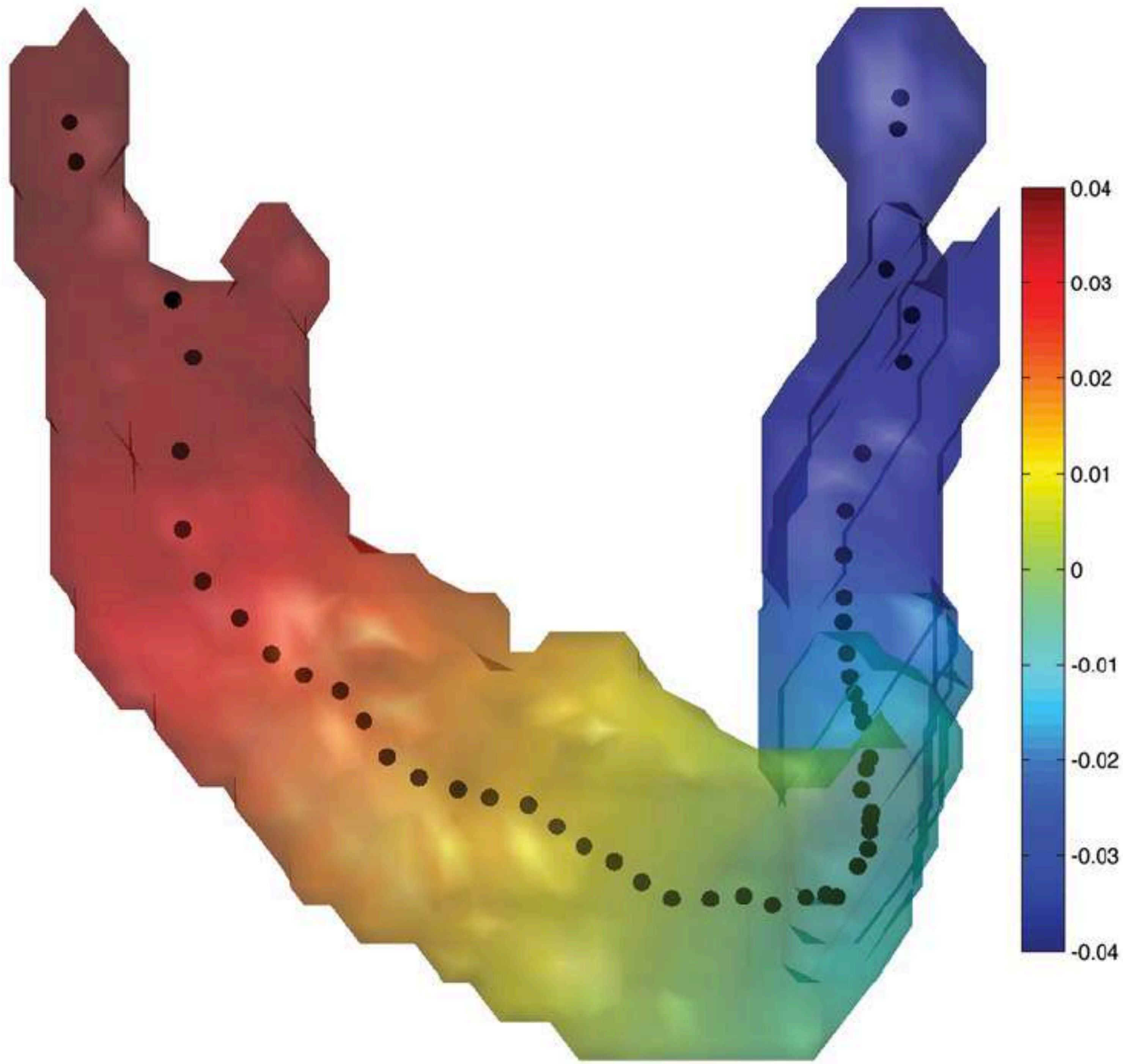

- heat sink

First attempt: diffusion with heat source and sink

Laplace-Beltrami eigenfunctions on mandible

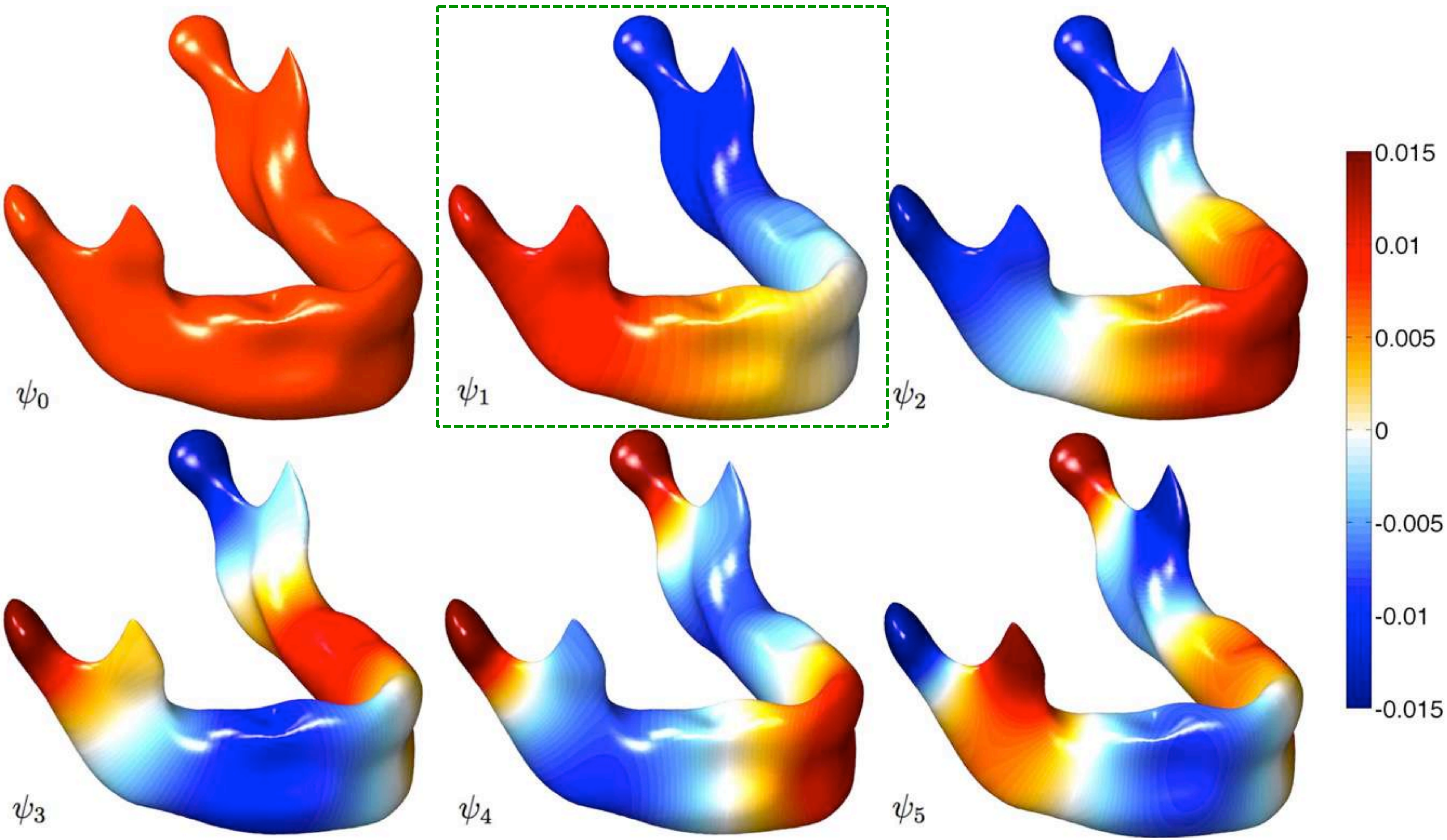

$$\Delta\psi_j = \lambda_j\psi_j$$

Rauch's hot spots conjecture unsolved since 1974

$$\frac{\partial f}{\partial t} = \Delta f, \;\; f(x, t=0) = X(x)$$

Neumann boundary condition

$$\frac{\partial f}{\partial n}(x,t) = 0$$

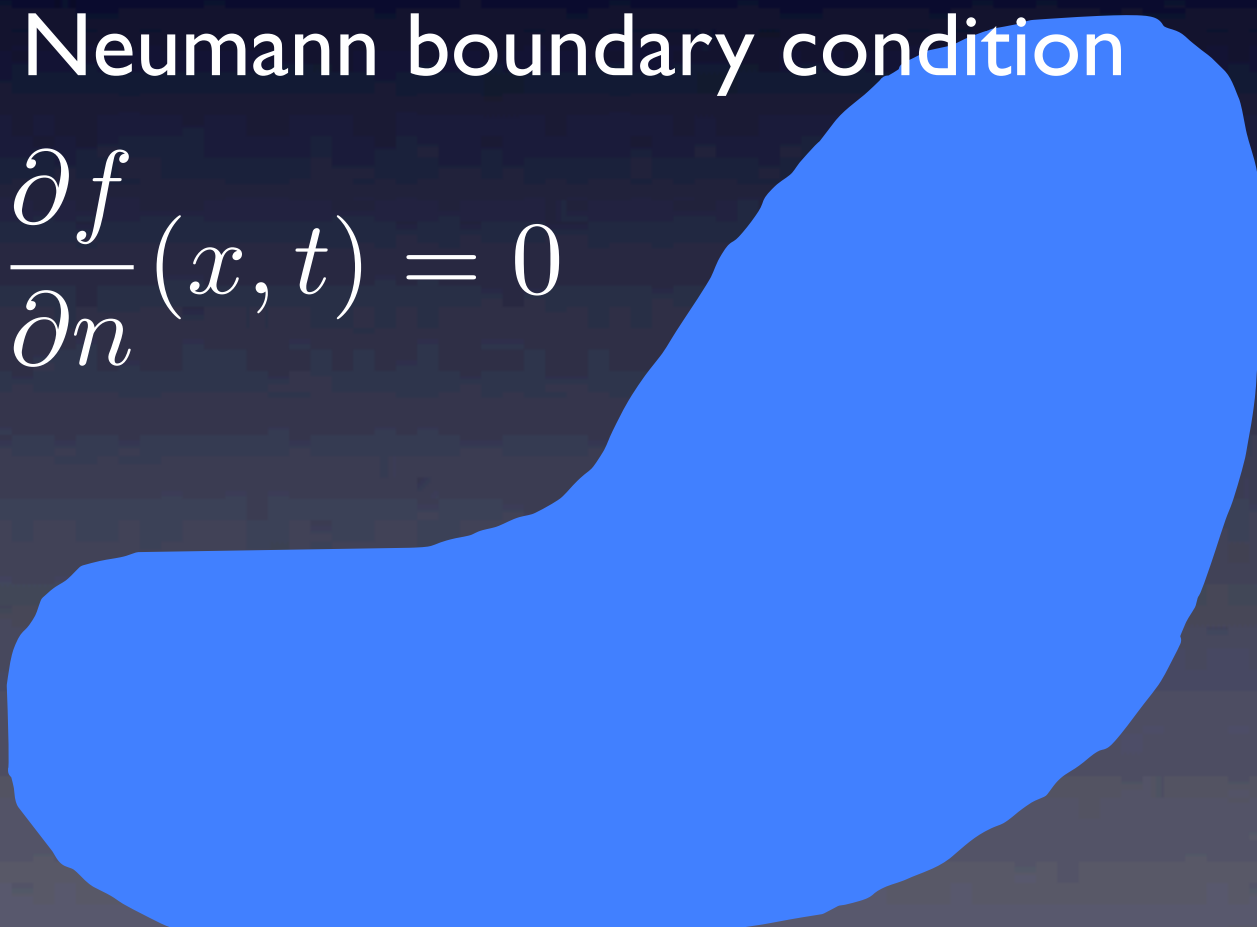

Conjecture:

The distance from the max/min of the solution to the boundary goes to zero as *t* goes to infinity.

Asymptotic property of diffusion

$$K_\sigma * f(p) = \frac{\int_{\mathcal{M}} f(p)\, d\mu(p)}{\mu(\mathcal{M})} + f_1 e^{-\lambda_1 \sigma} \psi_1(p) + R(\sigma, p)$$

Mean signal over manifold

Remainder

Restatement: The hot and cold spots of the second eigenfunction occur at the points that give the maximum geodesic distance.

Properties of Fidler vector on graphs

Hilbert nodal line theorem: The Fiedler vector partitions the node set into exactly two sign domains.

↓

Hot spot at the positive domain. Cold spot at the negative domain.

↓

Tlusty 2007 (Electronic Journal of Linear Algebra): The hot/cold spots have to occur at the boundary.

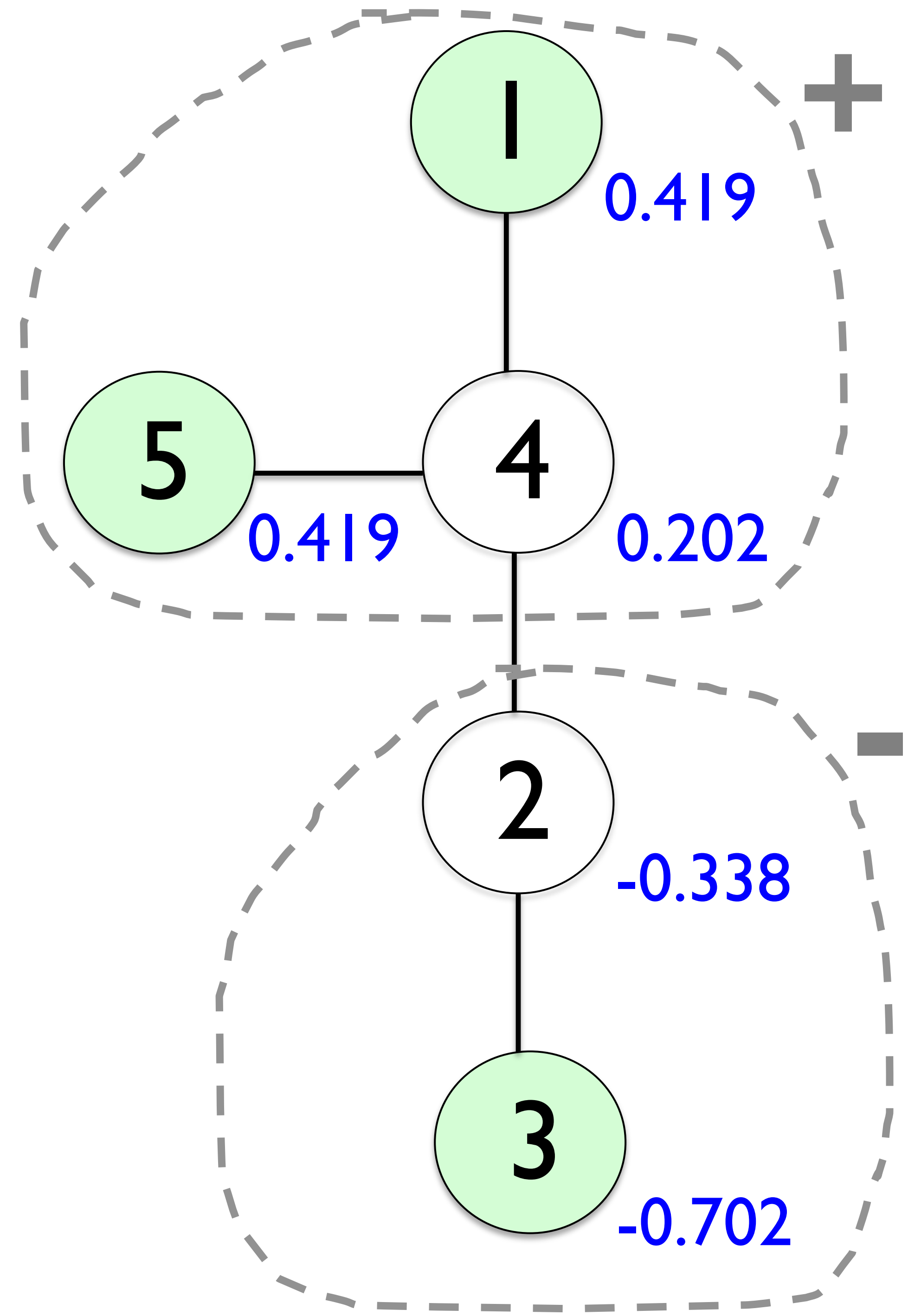

Example 3D surfaces

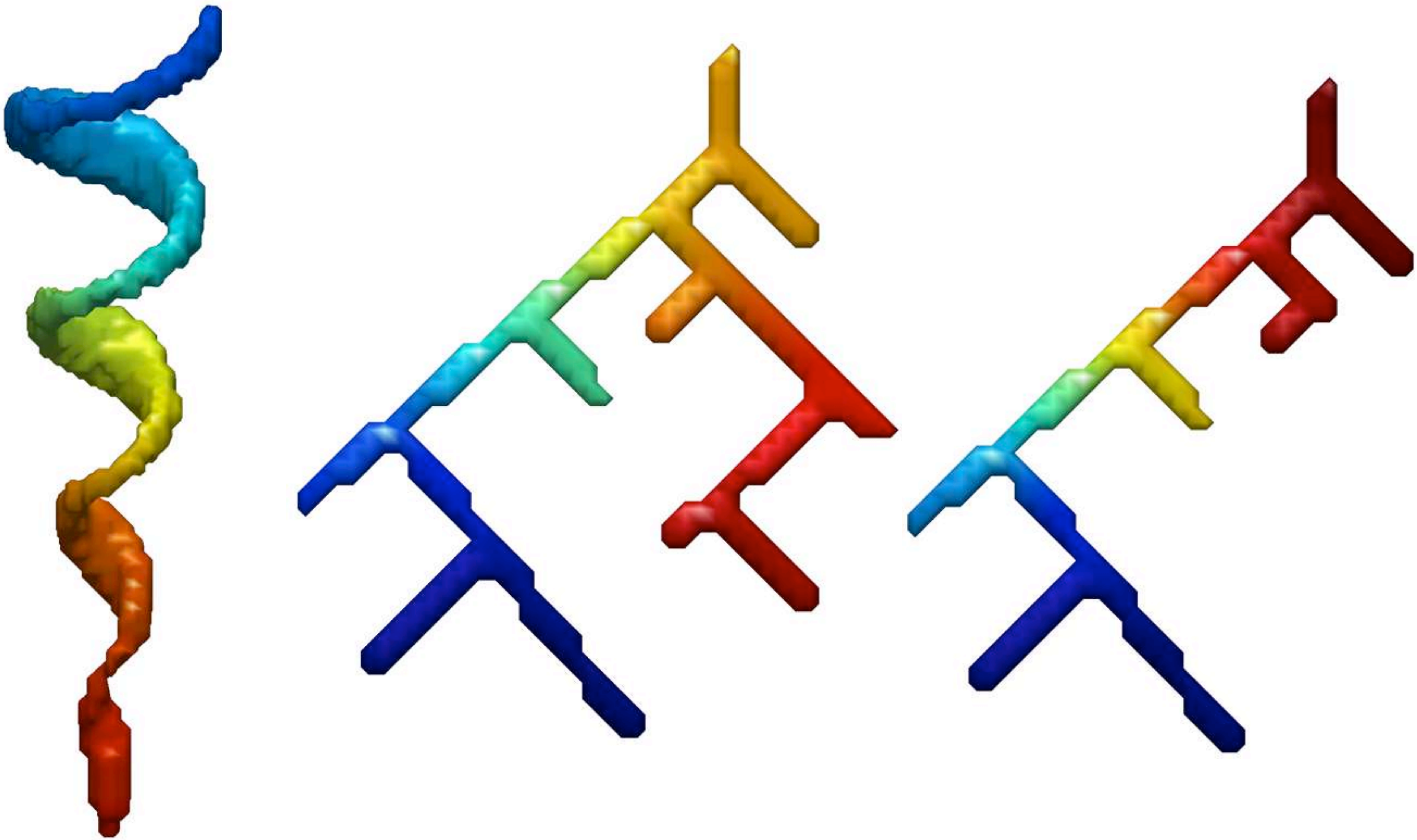

Tried more than 30 different objects: 2D, 3D trees, surfaces etc.

Second eigenfunction on trees

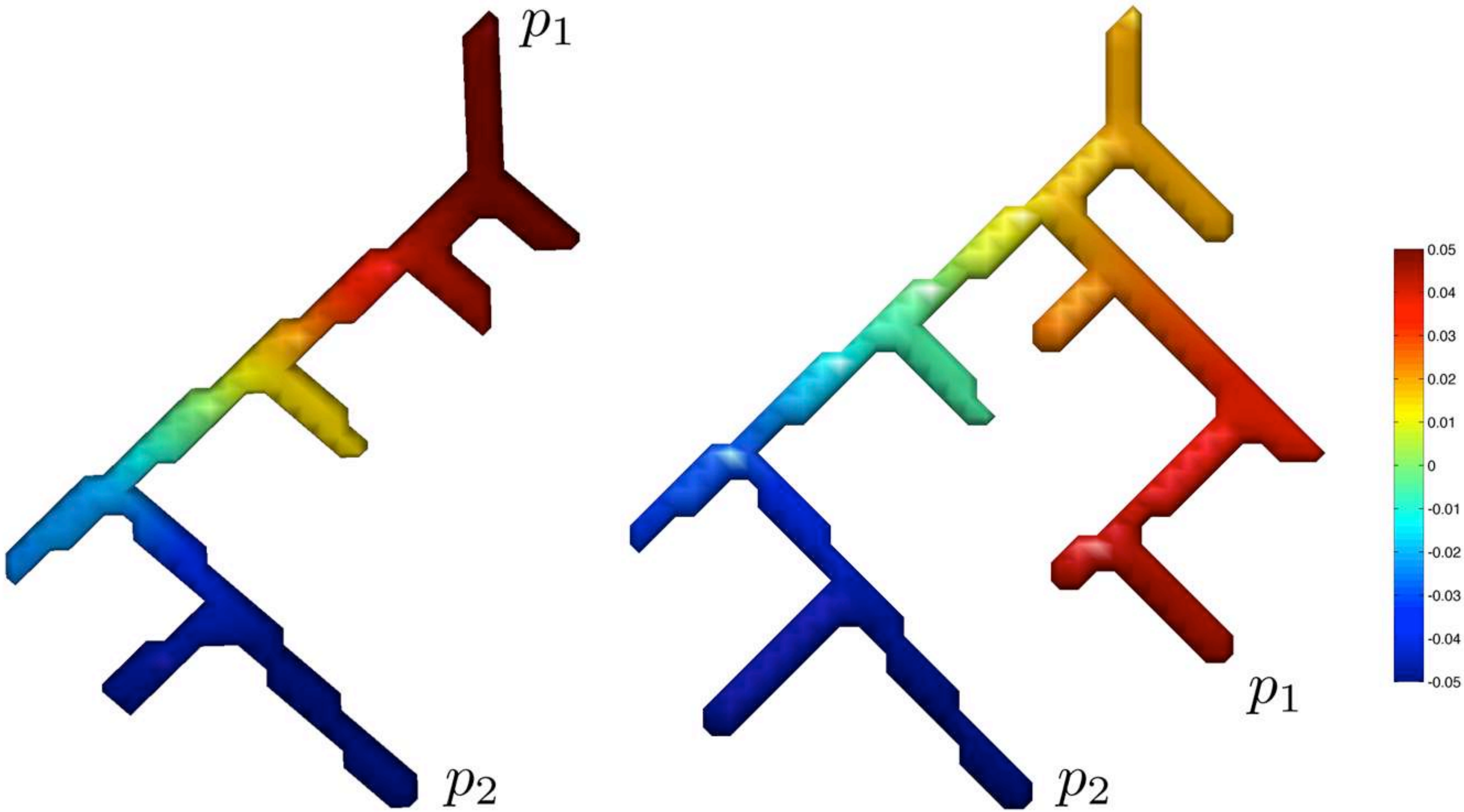

The topology/geometry aware 2nd eigenfunction

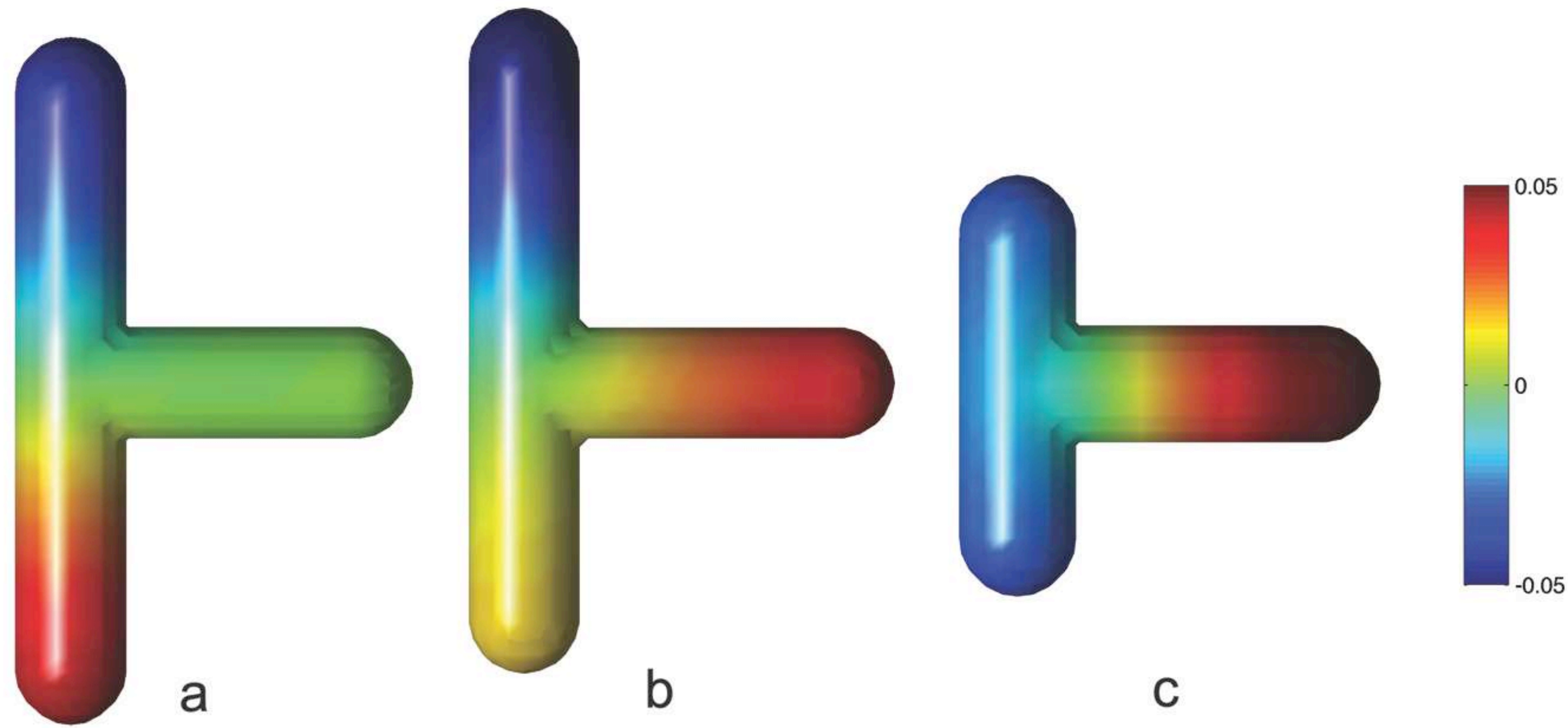

Can you guess where the max. and min of the 2nd eigenfunction will occur here?

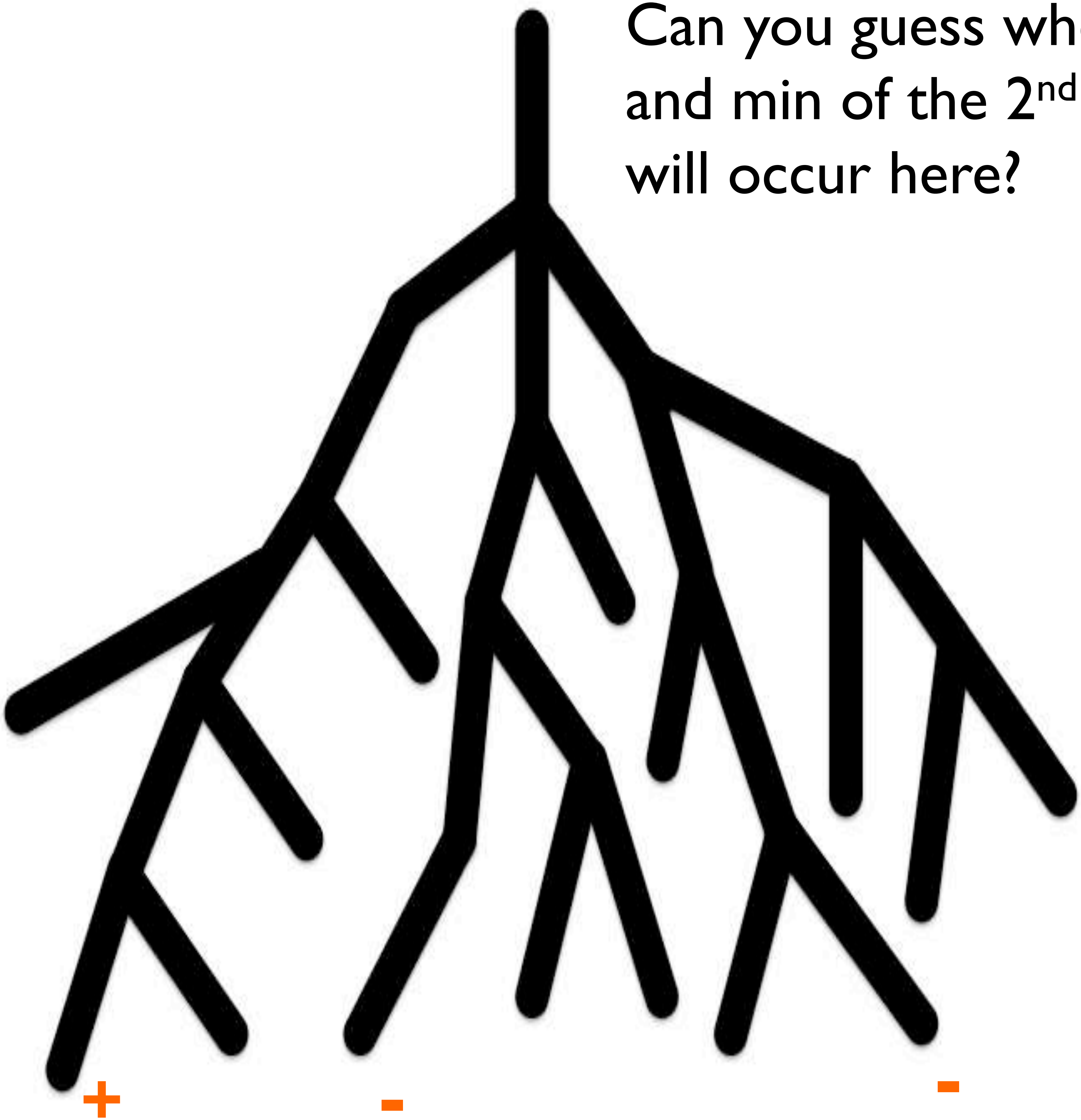

Applications

Centerline of mandible for 70 subjects

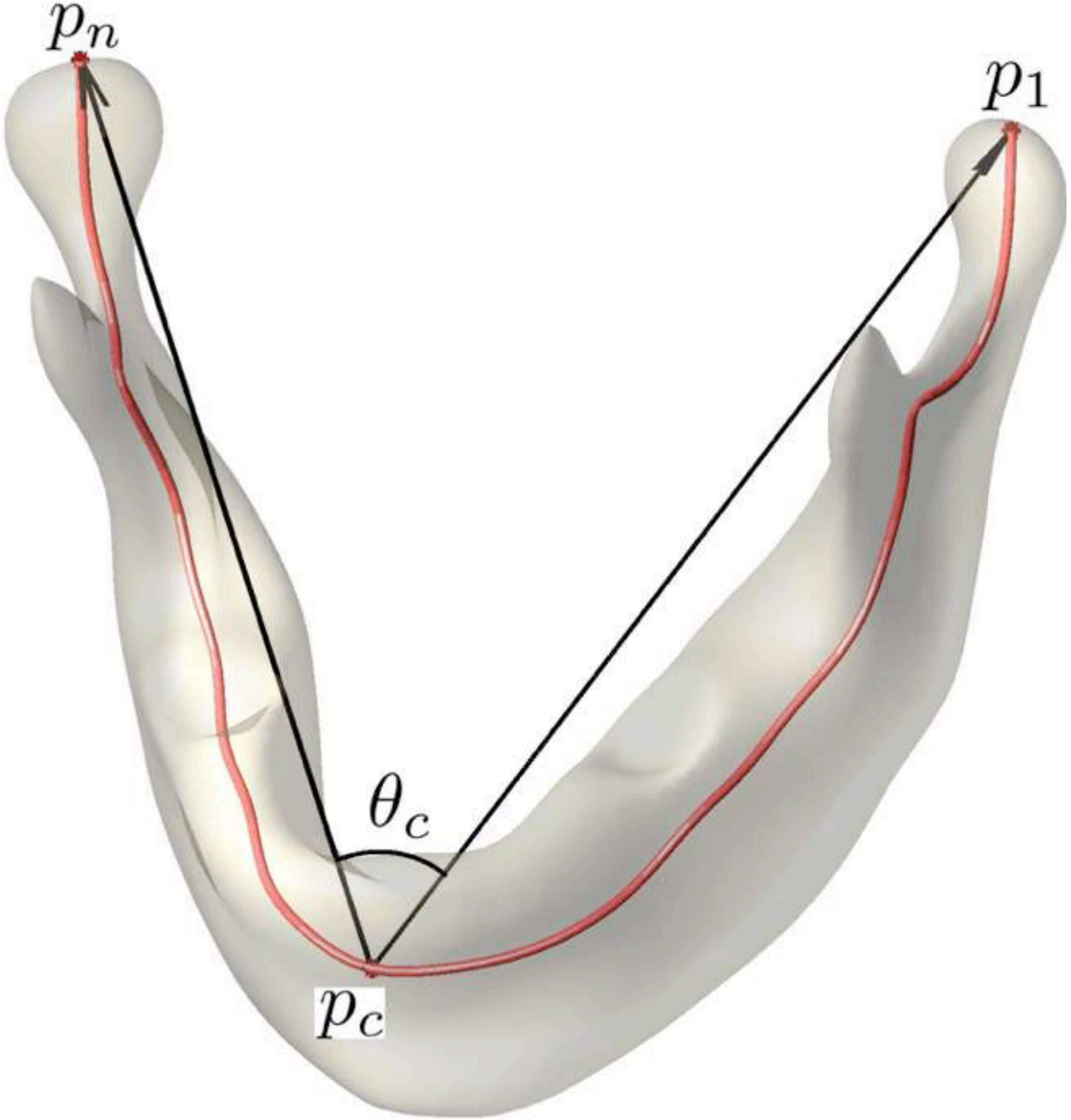

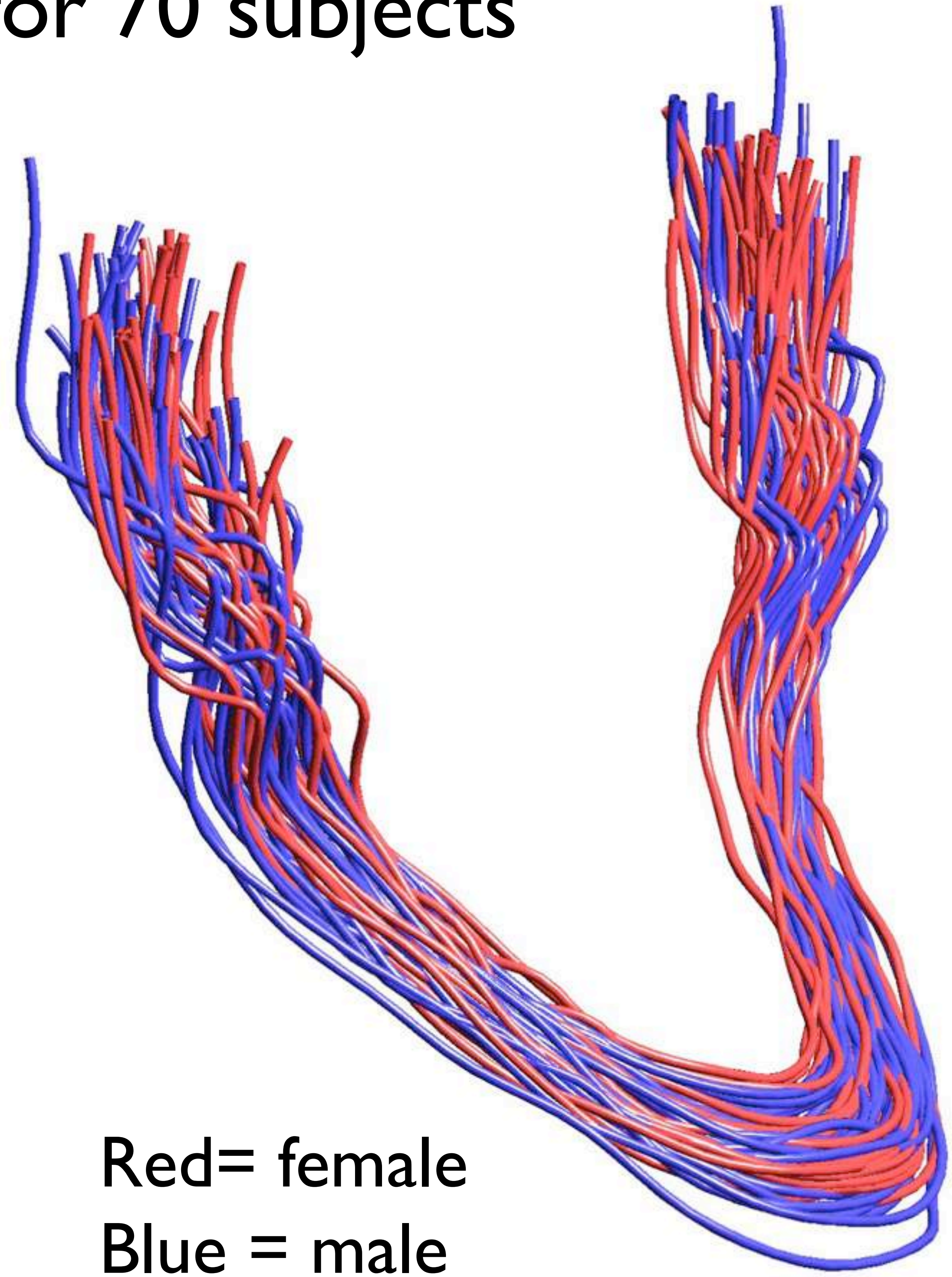

Elongation of mandible (length increases, angle decreases)

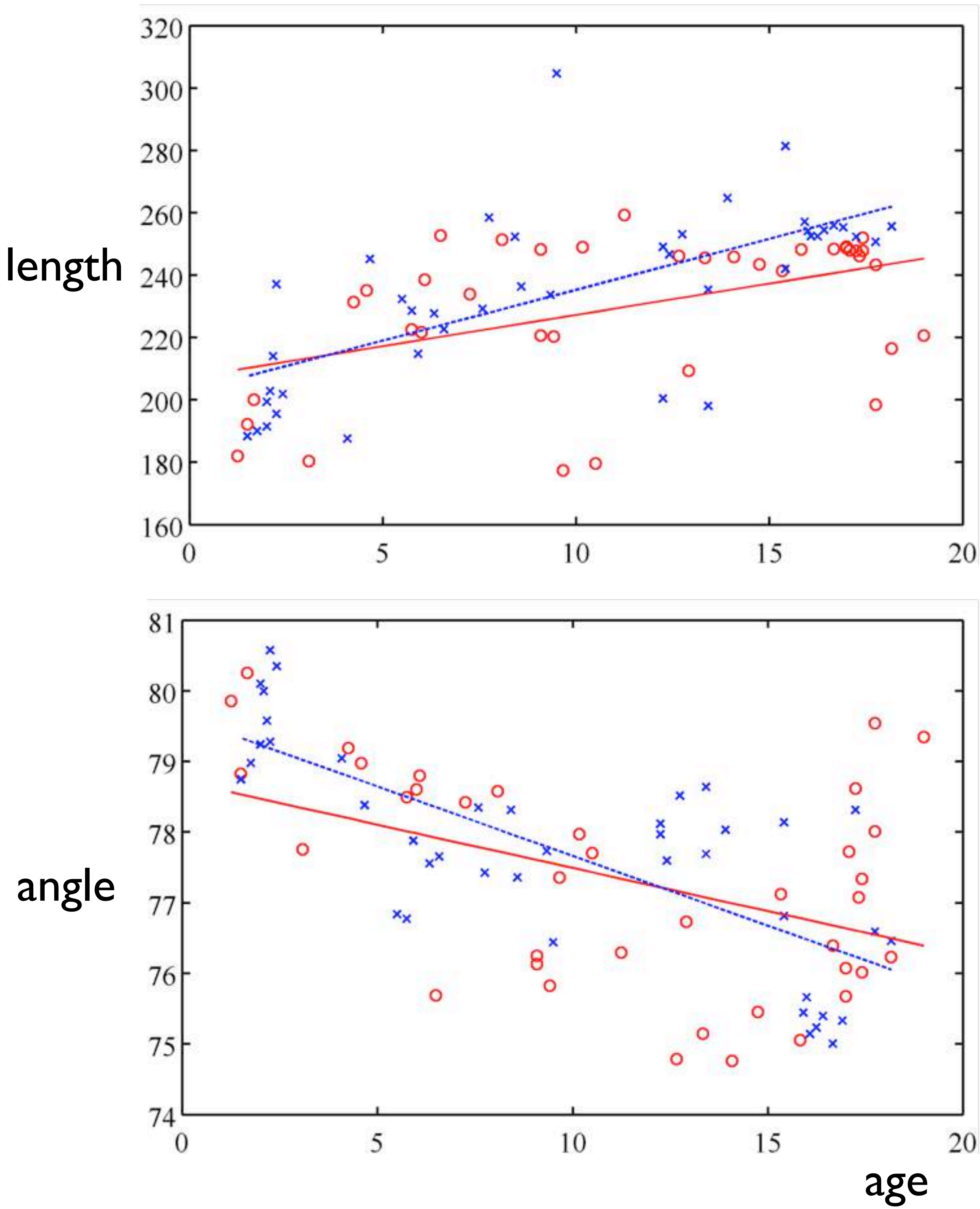

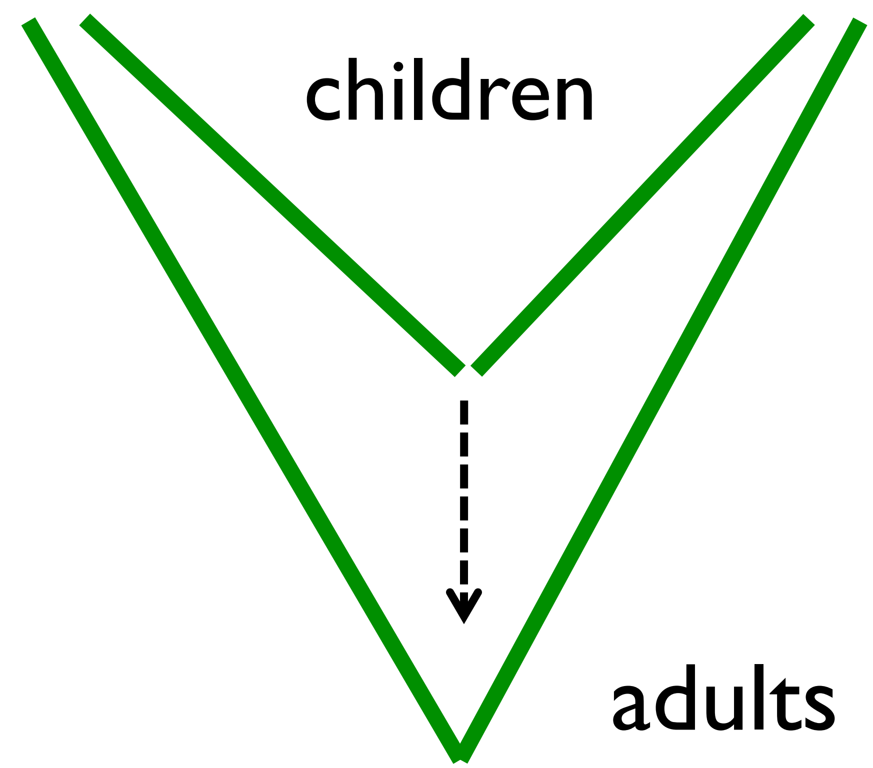

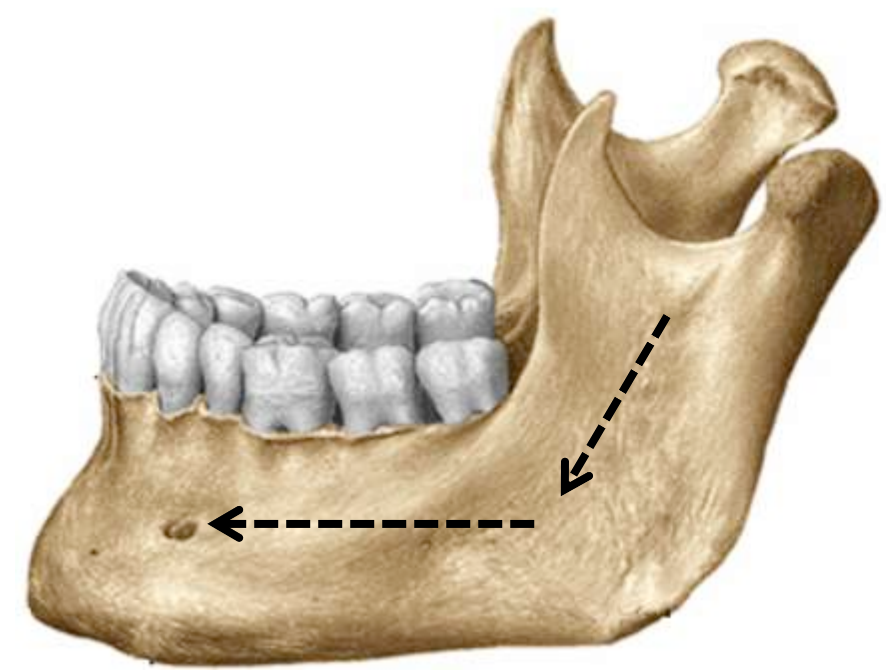

Diameter of a large-scale network

Diameter:
maximum of all possible shortest paths

Running time $O(n(n+e))$

Worst case $O(n^3)$

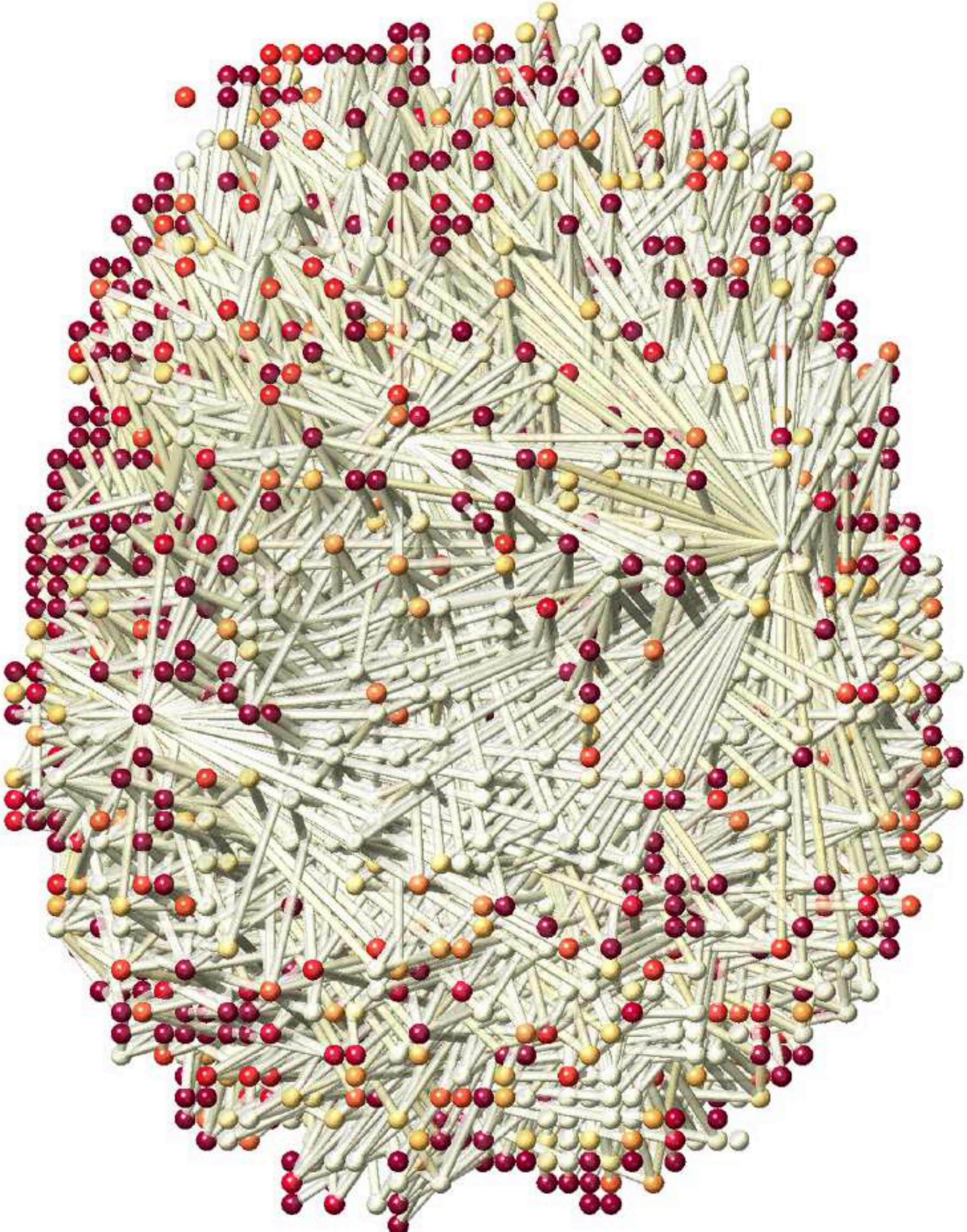

What next?

Persistent homology on hierarchical networks

Dense brain networks (fMRI correlation)

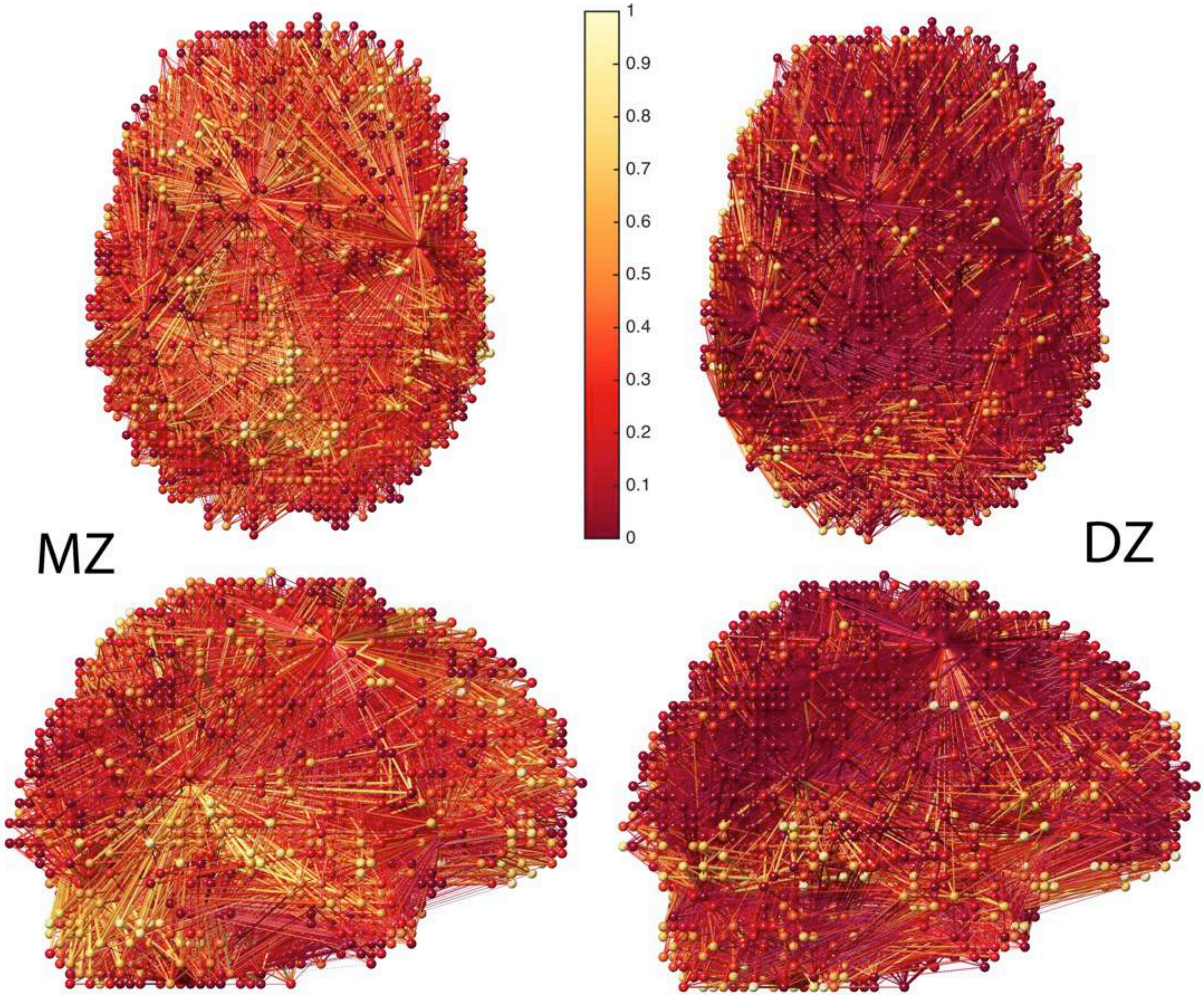

Hierarchical sparse network (compressed sensing)

Sparse model with sparse parameter λ :

$$S(\lambda)$$

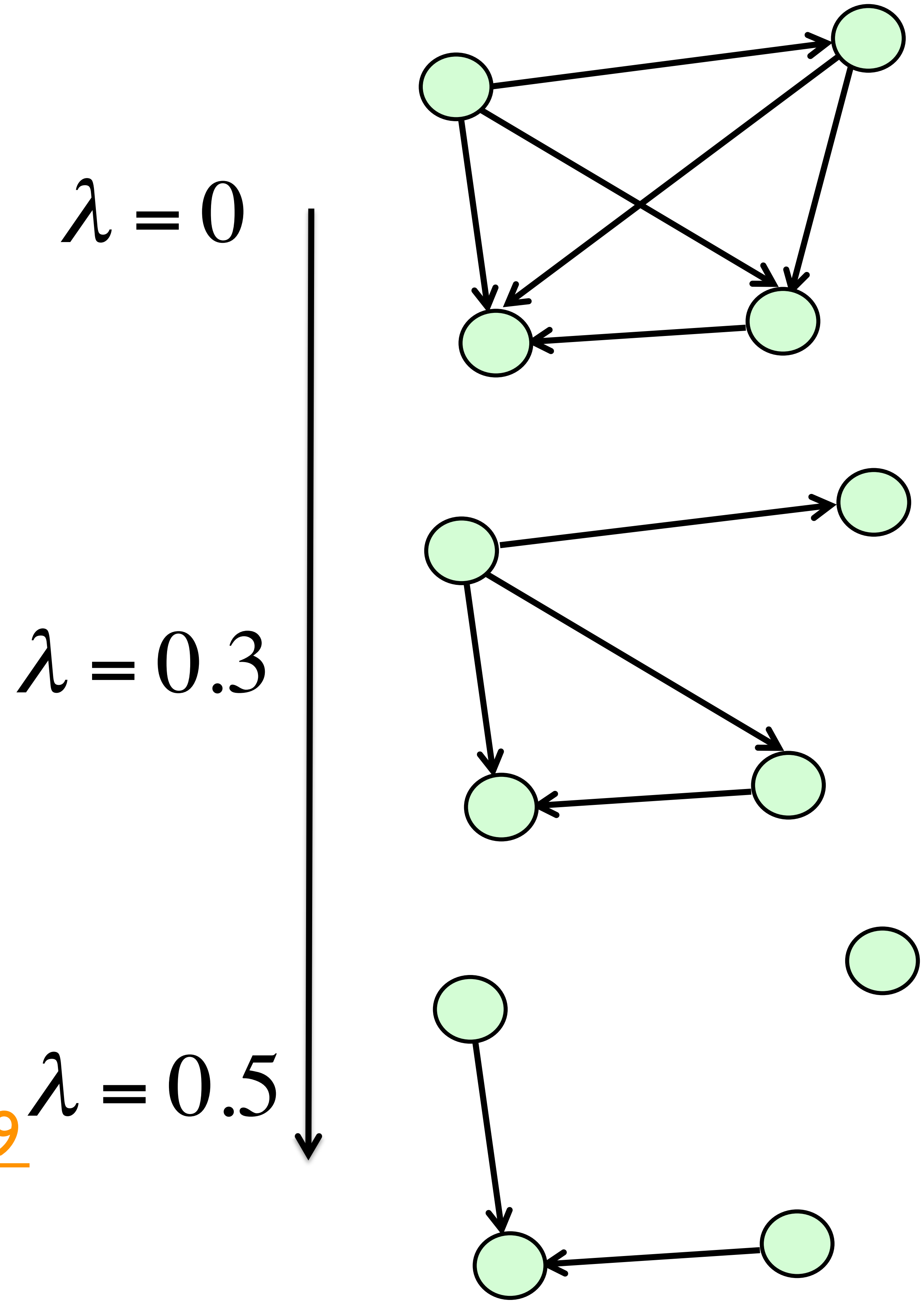

Undirected graph:

Chung et al. 2015 IEEE TMI 34:1928-1939

Directed graph:

Chung et al. 2017 IPMI 10265:299-310

Standard brain parcellation with 116 regions

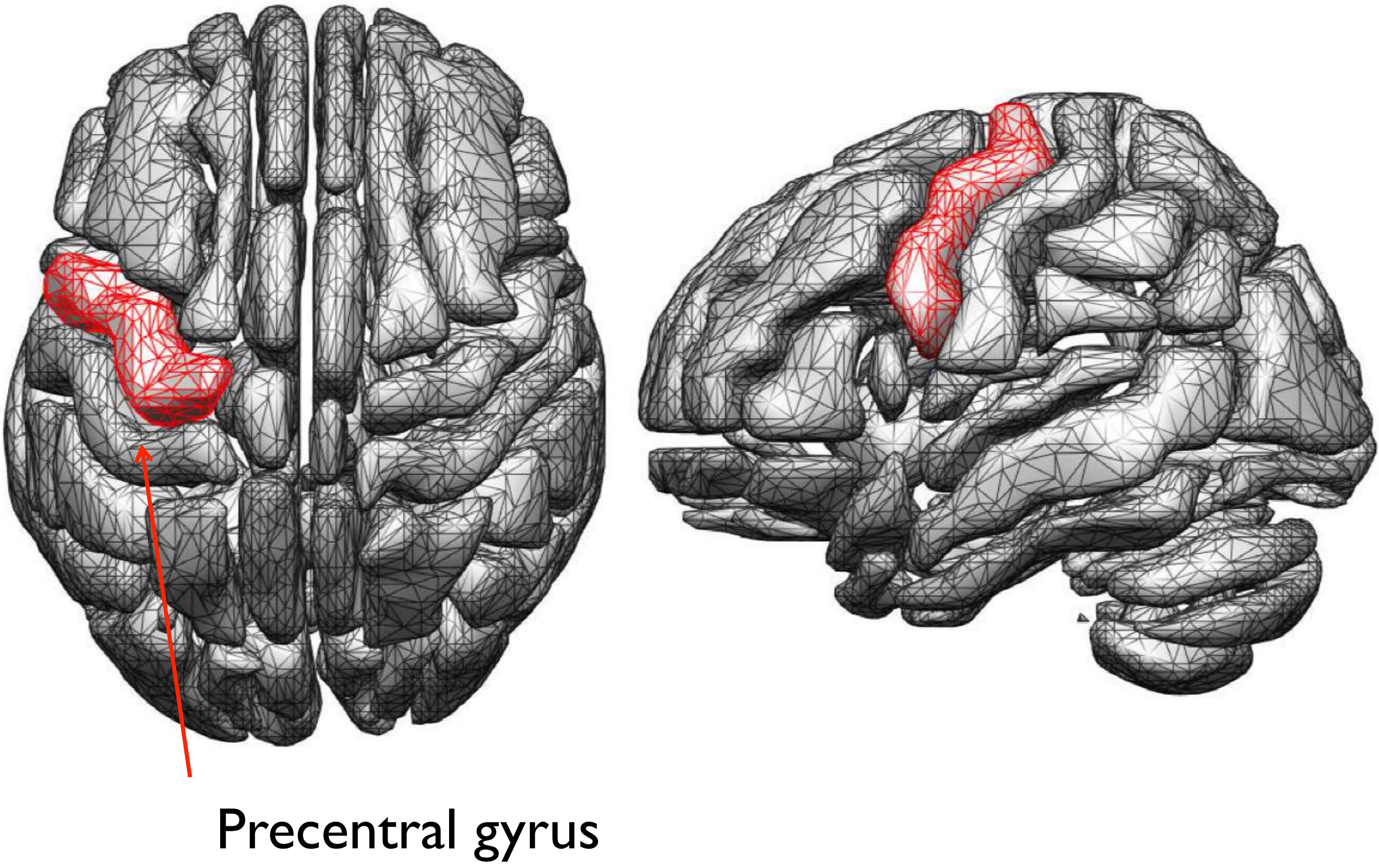

18-layer convolutional brain network

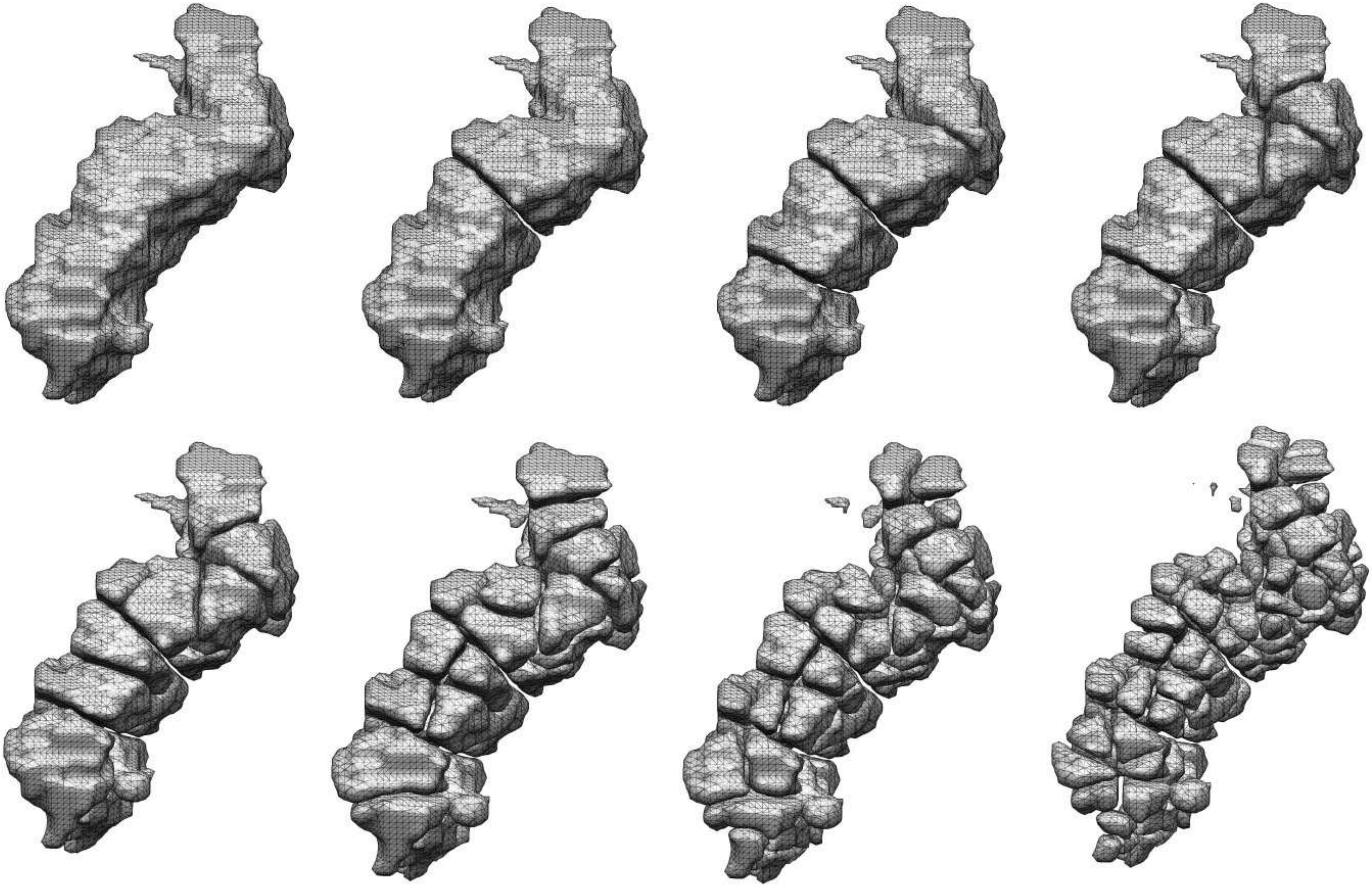

19-layer hierarchical brain parcellation

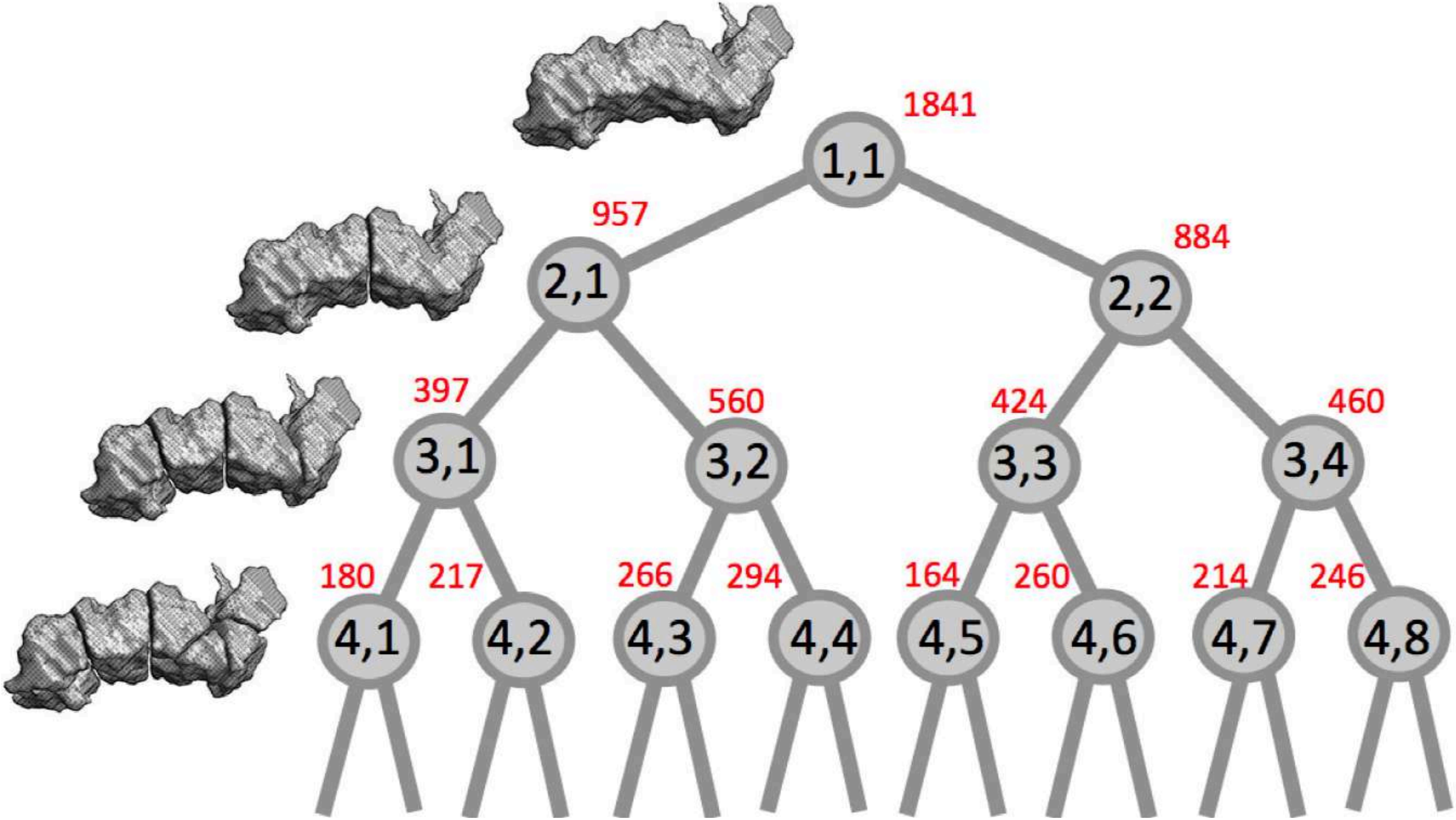

White matter fiber tracts

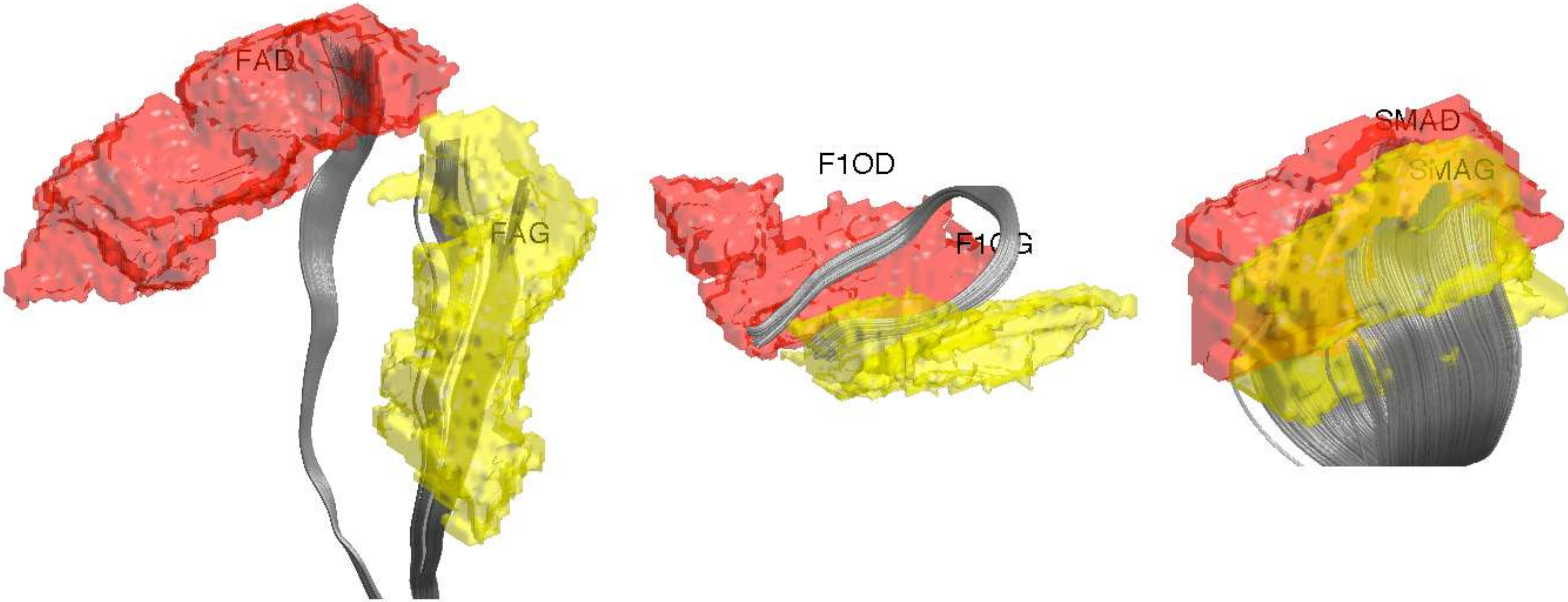

19-layer convolutional brain network